



Biosorption analysis of Cd(II) from industrial wastewater using endophytic bacterium *Agrobacterium tumefaciens* 12b3 by kinetic modeling and equilibrium studies

Razia Alam Gillani^{a,b}, Firdaus-e-Bareen^a, Naeem Ali^c, Hassan Javed Chaudhary^{b,*}

^aDepartment of Botany, University of Punjab, Lahore-54590, Pakistan, email: razziagillaniqau@gmail.com (R.A. Gillani), fbareen@gmail.com, firdaus.botany@pu.edu.pk (F.-e. Bareen)

^bDepartment of Plant Sciences, Faculty of Biological Sciences, Quaid-i-Azam University, Islamabad-45320, Pakistan, Tel. +92 51 90643004, Fax +92 51 90643096, email: hassaan@qau.edu.pk (H.J. Chaudhary)

^cDepartment of Microbiology, Quaid-i-Azam University, Islamabad, Pakistan, email: naemali2611@gmail.com (N. Ali)

Received 30 December 2017; Accepted 28 June 2018

ABSTRACT

Heavy metal pollution from industrial wastewater is a significant problem that can be solved through remediation. The present study investigated the adsorption capability of endophytic bacterium *Agrobacterium tumefaciens* 12b3 from the hyper accumulator plant *Oxalis corniculata* against Cd(II). Fourier transform infrared (FT-IR) technique was used for the surface characterization of the biosorbent and scanning electron microscopy (SEM) was applied to detect the change in biosorbent for adsorption of Cd(II) ions. Different factors such as pH, contact time and initial metal concentration for the adsorption of Cd(II) was studied in detail. Cd(II) was quantitatively adsorbed at pH 6 with optimum contact time of 30 min and adsorption increased as the concentration increased from 10 to 150 mg L⁻¹. The results were in accordance with Pseudo-second-order kinetic and Langmuir isothermal model with maximum capacity of 56.17 mg g⁻¹ of cadmium. The present study demonstrated that *A. tumefaciens* is quite efficient in adsorption of cadmium (II) and can open a new door in the field of remediation of heavy metals from industrial wastewater.

Keywords: *Agrobacterium tumefaciens*; Biosorption; Heavy metals; Equilibrium isotherms; Kinetic parameters

1. Introduction

Water pollution due to heavy metal contamination is a global environmental concern. Release of heavy metals into water without any proper treatment may cause many adverse effects on human health because of their toxic nature, persistence, biomagnification and accumulation throughout the food chain [1,2]. The main sources of heavy metal contamination of aqueous environment are effluents coming from various industries such as electroplating, metallurgical processes, mining, textile, storage batteries,

pigment, plastic manufacturing and fertilizers [3]. Among heavy metals cadmium, chromium, lead, manganese are highly toxic to environment and are not easily biodegradable [4]. Cadmium is the main cause of oxidative stress and cancer by binding to the necessary respiratory enzymes [5]. International agency for research on cancer declared cadmium as Category-I carcinogen. According to US environment protection agency cadmium(II) has been categorized as Group B1 carcinogen [6]. Exposure of cadmium to living organisms causes severe damage to various tissues and induces apoptosis in extensive variety of cell lines [7]. Cadmium induces single strand breaks in DNA, sister chroma-

*Corresponding author.

tid exchanges, chromosomal aberrations and damages the DNA-protein binding in various cells of organism [8].

Various conventional methods such as filtration, chemical precipitation, membrane technology, oxidation/reduction, electrochemical treatment, ion exchange, reverse osmosis, and evaporation recovery, have been used for removal of heavy metals from the contaminated water [9]. The main drawback of using these methods is that they are not cost effective, less efficient and more labor-intensive [10]. Nowadays more attention is being given on the use of microbial biomass, mainly bacteria for removal of heavy metals from contaminated water [11]. Biosorption is a combination of numerous mechanisms such as electrostatic attraction, complexation, Van der Waal's forces, ion-exchange, covalent binding, adsorption and microprecipitation [12]. During recent years, more importance has been given to biosorption technology due to its eco-friendly nature, better performance and cost-effectiveness. The major characteristics of microbial biomass that are involved in removal of heavy metals are membrane components, presence of functional groups, tolerance ability and uptake capacity [13]. There are a number of factors which affect the uptake ability of metals ions including temperature, pH, contact time and initial metal concentration [14]. Among these, pH is the major environmental factor that affects the solution chemistry and activity of functional groups in the microbial biomass [15]. The aim of this study is to find out the biosorption potential of *Agrobacterium tumefaciens* 12b3 against heavy metals in aqueous environment.

2. Materials and methods

2.1. Isolation and purification of endophytes

The endophytic bacterium *Agrobacterium tumefaciens* 12b3 was isolated from a wild plant *Oxalis corniculata* L. Samples of wild plant were collected from different spots of Quaid-i-Azam University Islamabad. Primary parts of the plant such as root, shoot and leaves were taken. The parts were cut into smaller pieces for the purpose of surface sterilization and then these parts were soaked into 3% hydrogen peroxide for approximately 4 min and after that these parts were washed with deionized water. HgCl_2 solution about 0.1% was also used for surface sterilization of different parts of plant tissues. Plant parts were soaked in 1 mL sterile distilled water and then shift into test tubes having 5 mL of Dobereiner nitrogen (DN) semisolid media. Test tubes were incubated for 7 days at $35 \pm 2^\circ\text{C}$ and then sub-cultured for further purification of bacterial growth according to method described by [16]. The strain was identified as *A. tumefaciens* based on 16S rRNA gene sequencing analysis with gene bank no. KF875446.

2.2. Preparation of biosorbent

The isolated strain *Agrobacterium tumefaciens* 12b3 was inoculated into 100 ml Luria-Bertani (LB) media containing 0.5 M NaCl in 250 mL conical flask and were incubated at 25°C for 48 h in an orbital shaker at 150 rpm. The cells grow till late exponential phase and were harvested by centrifugation at 4°C for 10 min at 4000 rpm in falcon tubes [17].

2.3. Formation of metal stock solution

Cadmium stock solution of 1000 mg L^{-1} was prepared by dissolving 1.791 g of cadmium chloride (CdCl_2) in 1 liter of double distilled water. The pH of the solution was set to different value such as (2, 4, 6, 8 and 10) by using diluted 0.1 M hydrochloric acid (HCl) for lowering pH value and 0.1 M sodium hydroxide (NaOH) to maintain basic pH. Different Cd(II) concentrations such as (10, 25, 50, 100 and 150 mg L^{-1}) were obtained by diluting the stock solution.

2.4. Batch adsorption studies

The batch adsorption experiment was conducted with different factors which can affect the biosorption process efficiently such as pH, adsorption time and initial metal concentration value. All the experiments were conducted in triplicate manner. The first factor which affects the biosorption process is pH. Five different values of pH 2, 4, 6, 8 and 10 were selected moving from highly acidic to basic. First of all 100 mL of metal stock solution was prepared in 250 mL Erlenmeyer flask with bacterial biomass of 0.5 g. Solutions were shaken at 150 rpm in orbital incubator shaker at temperature $35 \pm 2^\circ\text{C}$ for 60 min and were then centrifuged (4000 rpm) at 4°C for 10 min. The supernatant was collected for remaining cadmium concentration by using 240FS Varian Atomic Absorption Spectrophotometer. Same procedure was repeated for other parameters such as contact time and initial metal concentration as well. Metal removal by living cells of *Agrobacterium tumefaciens* 12b3 was determined according to the following equation.

$$q_e = \frac{C_o - C_e}{M} \times V \quad (1)$$

In this equation q_e (mg g^{-1}) is the cadmium ion adsorbed, C_o (mg L^{-1}) is the initial concentration of cadmium before sorption, C_e (mg L^{-1}) is the final concentration of cadmium after sorption, V (mL) is the volume of metal solution in the flask and M (g) is weight of biomass. The data was analysed by making comparison with control group.

2.5. Surface characterization by Fourier Transform Infrared Spectroscopy (FTIR)

The presence of effective groups on the surface of biosorbent were analysed by using FTIR spectroscopic technique. Approximately 1 mg of biosorbent material was mixed with about 100 mg of thinly separated spectroscopic Potassium bromide (KBr) disc. The fusion mix was hard-pressed beneath elevated pressure. Resulted discs were sited into Bruker Tensor 27 FTIR spectrometer and FTIR spectra were verified in the wave number ranging from $500\text{--}4000 \text{ cm}^{-1}$ [18].

2.6. Characterization of adsorbent using Scanning Electron Microscope (SEM)

In the present study SEM analysis (CASP-T) was done to detect any change in the surface morphology of bacteria after metal adsorption and to ensure the presence of metal ions on bacterial surface. Metal-loaded and metal free (control) microbial pellets were used for SEM analysis. Pellet

was treated with 4% glutaraldehyde in phosphate buffer (pH 6.9, 0.02 M) for 1 h and then wash with distilled water. Later, the pellet was washed with 10–100% alcohol, for 20 min at every step. Air dried the pellet and used for examination of SEM.

3. Results and discussion

3.1. Isolation and characterization of microorganisms

For the current study, isolated endophyte (*A. tumefaciens*) gram negative bacteria from root, stem and leaves of sterilized plant *Oxalis corniculata* was used with higher endophytic possession in leaves. The protein profile of isolated bacteria was determined by SDS-PAGE analysis. 16S *rRNA* gene sequencing of the isolate was performed and the strain showed 100% similarity with *Agrobacterium tumefaciens* (KF 875446).

3.2. Effect of pH on biosorption

The pH of the solution had important effect on the biosorption of heavy metals as it controls the magnitude of surface protonation of the sorbent and the degree of ionization. The concentration of hydrogen ions in the adsorption process is taken as one of the most noteworthy factors that affects the adsorption performance of metal ions in aqueous solutions. Fig. 1 shows adsorption of cadmium at different pH levels. The results revealed that maximum adsorption took place at 6 pH after which reduction in the process of adsorption occurred. At low pH, the total surface area of the cell appeared positively charged thus completion was created between metal cations and protons for adsorption sites on the cell wall and resulted in decrease in metal adsorption [19]. The presence of functional groups on the surface of cell get positively charged resulting in repulsion of metal such as cadmium and in the present case, this process occurred in acidic medium [20]. It is reported by different researchers that lower pH also affects the protonation of the cell wall components resulting in reduction in metal uptake by the bacterial biomass whereas with increase in pH values, the negative charge density increases over the cell surface that increase due to deprotonation of the metal attachment sites [21]. Moreover at high pH, the strength of hydrogen ions decreases making the cell wall more negatively charged.

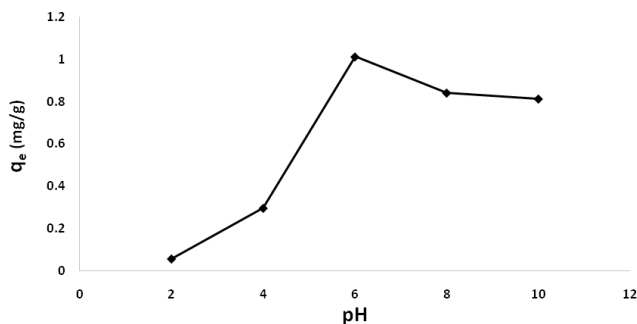


Fig. 1. Effect of pH of the solution on adsorption of Cd (II) onto *A. Tumefaciens* 12b3. At an initial metal concentration of 50 mg L⁻¹ and *A. tumefaciens* 12b3 dosage of 0.5 g L⁻¹ at 25°C.

This makes the attachment of Cd positive ions more efficient, therefore, it enhances the adsorption of metal ions [22]. But at pH higher than 8.0 adsorption was suppressed and precipitation can occur due to the formation of metal hydroxides [23]. The results were consistent with previous studies [19].

3.3. Effect of contact time on biosorption

Contact time is the main factor affecting the efficiency of biosorption. Optimum contact time is required to achieve the highest removal of metal ions. Equilibrium time is one of the significant factors for the treatment of wastewater [24]. Mostly the frequency of metal ion biosorption is higher in the start due to large availability of free metal ion binding sites on biosorbent but with the passage of time the rate of biosorption tends to slow down and finally reaches an equilibrium state. Zouboulis et al. [25] also observed that shortest time period of sorption is effective for higher removal of metal sorption. Similar results have also been determined by Gaber et al. [26] for Ni and Pb biosorption. The optimum contact time for this experiment was 30 min where maximum sorption occurred and after which the rate of the process became constant. All the available sites were filled by metal ions and no further sorption could take place as shown in Fig. 2.

3.4. Initial metal concentration

The concentration of metal plays a major role in the transfer of mass between the liquid and solid phases [27]. As the metal ion concentration increases in the solution, the electrostatic interactions between sorbent and sorbate also increase resulting in enhancement of metal sorption. When the concentration of metal is low all metal ions react with the active sites in the adsorbent with each active site being enclosed by many metal ions. Therefore at the start of reaction the uptake capacity is greater and as the concentration of metal increase the adsorption sites become saturated, so the adsorption also becomes constant as shown in Fig. 3. [28].

3.5. Langmuir isotherm model

The assumptions of Langmuir isotherm model is that the bacterial surface possesses homogeneous adsorption

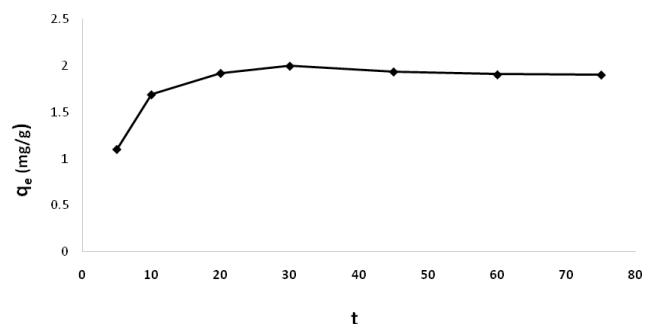


Fig. 2. Effect of contact time on adsorption of Cd (II) onto *A. tumefaciens* 12b3. At an initial concentration of 50 mg L⁻¹ and *A. tumefaciens* dosage of 0.5 g L⁻¹ at 25°C.

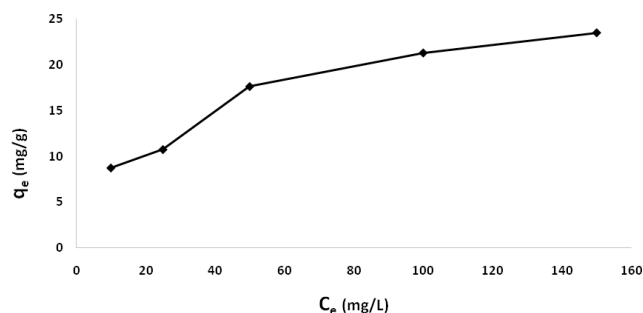


Fig. 3. Effect of metal concentration on adsorption of Cd (II) onto *A. tumefaciens* 12b3. At an initial concentration of 10, 50, 100 and 150 mg L⁻¹. *A. tumefaciens* 12b3 dosage of 0.5 g L⁻¹ at 25°C.

sites with equal distribution of energies [29]. The monolayer adsorption model offers the maximum adsorption capacity Q_{max} . The equation of Langmuir adsorption isotherm is given below.

$$\frac{1}{q_e} = \frac{1}{Q_{max}} + \frac{1}{Q_{max} b C_e} \quad (2)$$

where C_e (mg L⁻¹) is the concentration of metal ion at equilibrium, q_e (mg g⁻¹) is the adsorption capability over equilibrium position, Q_{max} (mg g⁻¹) is the maximum adsorption capacity and b is the adsorption energy constant at equilibrium (L mg⁻¹) which quantitatively reflects the attraction between *A. tumefaciens* 12b3 and metal ions. Graphs of $1/q_e$ versus $1/C_e$ produced straight line for metal ions (Fig. 4) which prove that the adsorption is uniform. Q_{max}/b and correlation coefficient (R^2) were calibrated from the graphs.

R_L is dimensionless factor relating the efficacy of sorption and is written by the equation as follow:

$$R_L = \frac{1}{1 + b \times C_o} \quad (3)$$

where C_o (mg L⁻¹) is the initial metal ion concentration and b (L⁻¹ mg) is Langmuir constant. R_L values ranging from 0–1 shows the effectiveness of adsorption phenomena. R_L value of Cd (II) is 0.048. This indicates a highly favourable adsorption of Cd (II) onto *A. tumefaciens*12b3.

3.6. Freundlich isotherm

Non-linear sorption model based on the hypothesis that the adsorbent is structurally heterogeneous with all adsorption sites that are actively different in energy level. The adsorption from diluted solutions is specified by Freundlich model as [30]. The equation of Freundlich adsorption isotherm model is represented below.

$$\log q_e = \log K_f + \frac{1}{n} \log C_e \quad (4)$$

where K_f is adsorption ability and n is adsorption strength both are Freundlich constants which are to be measured. Plots of $\log q_e$ versus $\log C_e$ yielded straight lines for Cd (II) adsorption on *A. tumefaciens*12b3 (Fig. 5).

The Langmuir model was most suitable against adsorption information (R^2 , 0.9302 for Cd(II)) than Freundlich

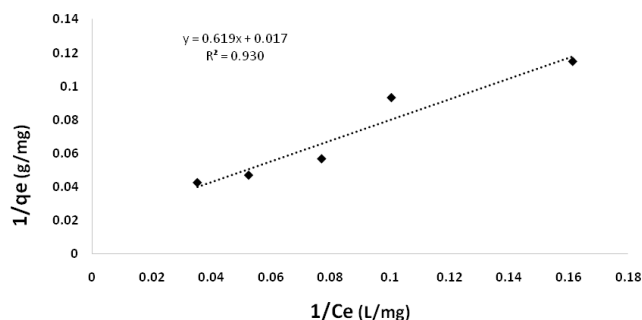


Fig. 4. The Langmuir adsorption isotherm for Cd (II) adsorption onto *A. tumefaciens* 12b3.

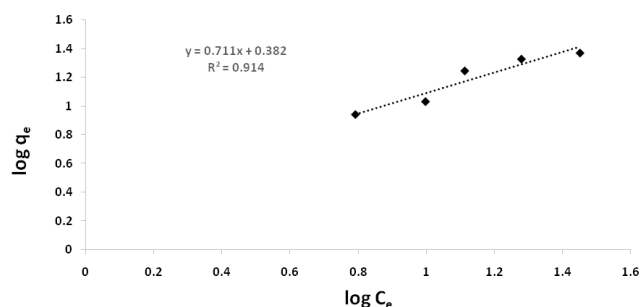


Fig. 5. The Freundlich isotherm for Cd (II) adsorption onto *A. tumefaciens* 12b3.

Table 1
Isotherm constants and coefficients of Langmuir and Freundlich models

Adsorbate	Langmuir models			Freundlich models		
	Q_{max} (mg g ⁻¹)	b (mg L ⁻¹)	R^2	K_f	n	R^2
Cd (II)	56.17	0.028	0.9302	2.4099	0.7116	0.9144

Q_{max} = maximum metal ions adsorption capacity of biosorbent, b = energy constant, K_f = binding constant, n = intensity of adsorption, R^2 = correlation coefficient

model (R^2 , 0.9144 for Cd(II)) in the range of concentration 10–150 mg L⁻¹ as shown in (Table 1).

3.7. Kinetics of adsorption

The adsorption of cadmium ions by *A. tumefaciens* depends on the contact time, Therefore the study of the kinetics models is a significant factor.

3.7.1. Pseudo-second order of kinetic modelling

The pseudo-second order equation is considered a particular kind of Langmuir kinetics [31]. The pseudo second order model is dependent on the fractional filling up of surface of adsorbent by adsorbate molecules adsorbed at any time than to the amount of adsorbate adsorbed at equilib-

rium. The adsorption sites are deep within the tiny pores so it may become gradually difficult for the adsorbate particles to reach them. Similar results were obtained by Hubbe et al. [32]. Several studies have been reported that most acceptable model for metal sorption kinetics is pseudo-second order [33,34]. The pseudo-second order kinetic equation is given as [35].

$$\frac{t}{q_t} = \frac{1}{k_2 q_e^2} + \frac{t}{q_e} \quad (5)$$

where q_t and q_e (mg g^{-1}) is the quantity of metal ions adsorbed at time 't' (min) and k_2 (g/mg/min) is the pseudo second order rate constant. A graph t/q_t versus t will give a straight line. The values of k_2 and q_e are measured from graph by the values of intercept and gradient, respectively.

The initial rate of adsorption, h ($\text{mg g}^{-1} \text{min}^{-1}$), is calculated from the equation given below.

$$h = k_2 q_e^2 \quad (6)$$

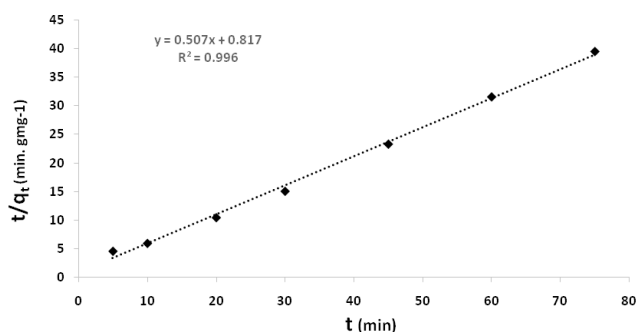


Fig. 6. The pseudo-second-order model for Cd (II) adsorption onto *A. tumefaciens* 12b3. At 25°C, 0.5 g L⁻¹ dosage and pH 6.

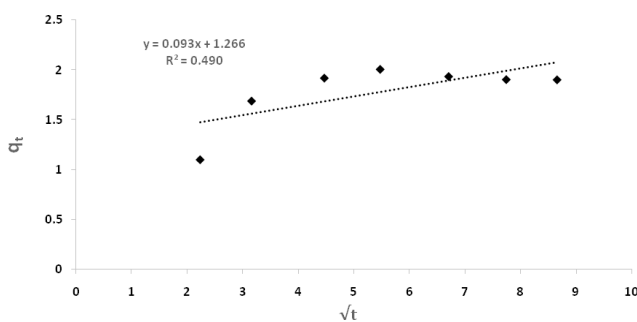


Fig. 7. The intra-particle diffusion model for Cd (II) adsorption onto *A. tumefaciens* 12b3. At 25°C, 0.5 g L⁻¹ dosage and pH 6.

The value of k , q_e , h and correlation co-efficient R^2 of pseudo-second-order kinetics are listed in (Table 2)

3.7.2. Intra-particle diffusion model

Weber-Morris has given the concept of Intra-particle diffusion model. He observed that uptake of solute particles varies proportionately with $t^{1/2}$ rather than with the t contact time in many adsorption processes [36].

$$q_t = k_{int} t^{1/2} \quad (7)$$

where k_{int} is the intra-particle diffusion rate constant. A graph of q_t vs $t^{1/2}$ should represent a straight line and must pass through the origin with a slope k_{int} when the rate-limiting step is intra-particle diffusion. The equation can be modified as [37].

$$q_t = k_{int} t^{1/2} + C_i \quad (8)$$

where k_{int} ($\text{mg/g/min}^{1/2}$) is intra-particle diffusion rate constant and C_i (mg g^{-1}) is intercept which describes the thickness of the boundary layer.

3.8. FT-IR spectral analysis

FT-IR is a vital tool that is used for the identification and characterization of functional groups present over the cell wall surface of the biosorbents. In the present study, the FT-IR spectra of Control (without metal) *Agrobacterium tumefaciens* 12b3 and metal loaded sample (Cd II) was examined by this technique in the range of 400–4000 cm^{-1} . As each bacterium has unique and special characters and a single bacterium could be checked through Fourier transform infrared (FTIR) spectrum [38]. FT-IR spectra of metal loaded and unloaded showed different kind of absorption peaks in the spectrum which are represented by different functional groups located over the cell surface. Pwan et al. [39] suggested that following functional groups are mainly responsible for a biosorption mechanism such as hydroxyl, carbonyl, carboxyl, amide, sulfonate, imidazole and phosphodiester groups. Range and pattern of different peaks along with their functional groups are presented in the table which also shows the banding and stretching of certain peaks due to the effect of heavy metal as in the present case of cadmium. The range from 3200–3250 cm^{-1} refers to hydroxyl and amino groups which are responsible for the binding of metal to the cell wall [40]. In recent analysis the peaks shifted from 3320.17 to 3318.79 cm^{-1} which also indicate the stretching of O-H and N-H group due to the binding of metal cation cadmium. The absorption peaks

Table 2

Pseudo-second order and intra-particle diffusion models for the adsorption of Cadmium ions

Adsorbate	Pseudo-second-order			R^2	Exp. value $q_{e,exp}$ (mg g^{-1})	Intra-particle diffusion		
	$q_{e,cal}$ (mg g^{-1})	k_2 ($\text{g mg}^{-1} \text{min}^{-1}$)	h ($\text{mg g}^{-1} \text{min}^{-1}$)			K_{int} ($\text{mg g}^{-1} \text{min}^{-1/2}$)	C_i (mg g^{-1})	R^2
Cd(II)	1.97005	0.3151	1.2569	0.9969	1.9974	0.0933	1.2667	0.4903

q_e = at equilibrium adsorption capacity; k_2 = pseudo-second order rate constant; h = initial adsorption rate; R^2 = correlation coefficient; K_{int} = intraparticle diffusion rate constant; C_i = thickness of boundary layer; R^2 = Correlation coefficient.

Table 3
Range of FTIR spectra with respect to functional groups involve in biosorption process

Wave number peaks (cm ⁻¹)				
Range of IR- Spectra	<i>Agrobacterium tumefaciens</i> 12b3	Metal loaded (Cd)	Functional groups	References
3200–3520	3320.17	3318.79	O-H and N-H stretching	[40]
2800–3000	2994.71	2994.72	C-H asymmetric stretching (alkenes)	[46]
2700–2900	2831.97	2831.81	CH ₃ -CH ₂ asymmetric and symmetric stretching	[43]
1400–1600	1449.67	1449.79	C-O symmetric stretching of carboxyl, amino acids and fatty acids.	[44]
1000–1100	1023.18	1023.27	P-O symmetric stretching of phosphodiesteres.	[47]
500–700	664.28	666.78	C-O, C-C and C-N mostly known as finger print region.	[38]

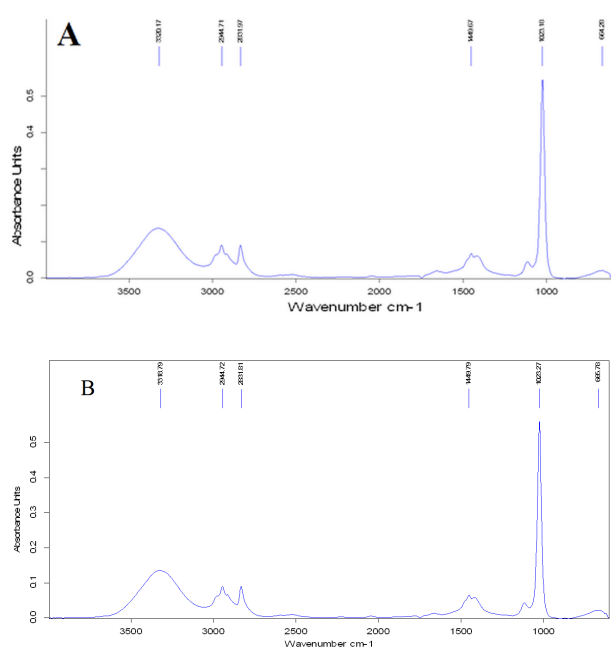


Fig. 8. FTIR spectra of *Agrobacterium tumefaciens* 12b3 (a) without metal stress (b) with Cd(II) metal stress.

nearly equal to 2800–3000 cm⁻¹ are referred to as asymmetric C-H stretching in fatty acids of bacterial cell membranes [41]. The peak at 2944.71 cm⁻¹ can be assigned to C-H stretching of alkene groups and it shifted with slight change in the peak giving value of wave number 2944.72 cm⁻¹ after cadmium adsorption in the endophytic *Agrobacterium tumefaciens* 12b3. Our present study correlates with pervious findings of FT-IR with different biosorbents [42]. The peaks in the range of 2700–2900 either belong to CH₃ or CH₂ groups which lead to asymmetric and symmetric stretching of these groups [43]. So the peak changed minutely from 2831.97 to 2831.81 cm⁻¹ due to cadmium adsorption. The peaks ranging from 1400–1600 cm⁻¹ belong to fatty acids and amino acids. This range also indicates the symmetric stretching of carboxyl group [44]. The stretching and shifting in the present case take place from 1449.67–1449.79 cm⁻¹. The shift from 1023.18 to 1023.27 is the indicative of C-N stretching of amino groups and may also be related P-O-C links of the organic phosphate groups [45]. Changes in peaks compared to the control cells were

observed in the 500–700 cm⁻¹ range after metal was loaded. According to previous studies, this range is a fingerprint region that is specific for every bacterium and is related to less well-known components of the cells [38].

3.9. Scanning electron microscopy analysis of metal stress and without metal stress of biosorbent

The surface morphology of Cd (II) loaded and unloaded *A. tumefaciens* was examined using scanning electron microscopy (SEM) at functional voltage of 20 kV. (Figs. 9 and 10). The scanning electron micrograph clearly showed the surface texture and morphology of the biosorbent at 2000x magnifications. The morphological changes in the biosorbent that is shiny and bright in appearance is indicative of effective interaction of Cd(II) on to the bacterial surfaces. The bacterial surface appeared as dense homogeneous surface after interaction with Cd(II). Fig. 10 explains the bulky and shiny appearance of surface being covered with Cd(II) ions. Similar results were observed by Rajesh et al and Arivalagan et al. [48,49].

4. Comparison with other biosorbents

The adsorption capacity of *A. tumefaciens* 12b3 was compared with other biosorbents. The comparison indicates that *A. tumefaciens* 12b3 has good adsorption capacity as compared to other biosorbents (Table 4). Thus, it can be concluded that *A. tumefaciens* 12b3 is quite effective in binding Cd on its surface.

5. Conclusion

The present study describes the adsorption potential of *A. tumefaciens* 12b3 isolated from the plant *Oxalis corniculata*. The attachment of metal ions to the surface of adsorbent take place due to the presence functional groups. These functional groups are responsible for metal binding on to the adsorbent and removal from wastewater. The results reveal that the process of adsorption changes with the change in pH, contact time and initial concentration of metal. The process of adsorption proliferates with the increase in the pH value up to 6 for Cd(II) and then it start decreases. The process of adsorption is improved with the

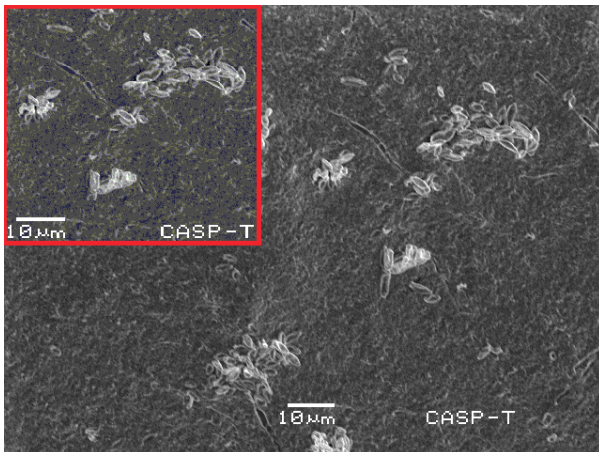


Fig. 9. SEM images of biosorbent before metal adsorption. (Acc. V = 20.0 KV; Magn = 2000×).

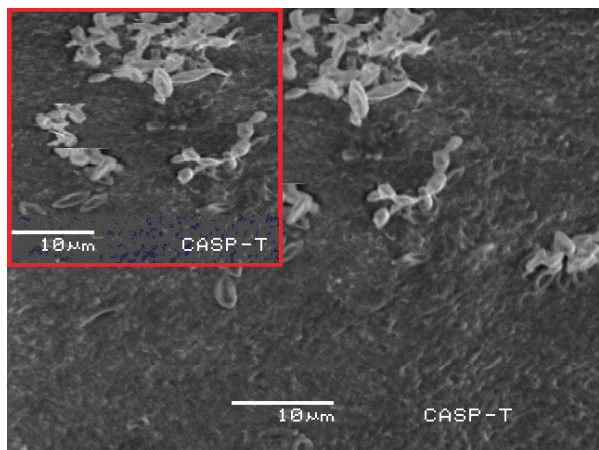


Fig. 10. SEM images of biosorbent after metal adsorption. (Acc. V = 20.0 KV; Magn = 2000×).

Table 4
Comparison of *A. tumefaciens* for Cd biosorption with other sorbents

Biosorbent	Metal	Q_{max} (mg g^{-1})	Refs.
<i>Saccharomyces cerevisiae</i>	Cd(II)	8.17	50
<i>Anoxybacillus amylolyticus</i>	Cd(II)	18.72	51
<i>Spirogyra hyalina</i>	Cd(II)	18.18	52
<i>Rhodococcus opacus</i>	Cd(II)	1.55	53
<i>Mucor rouxii</i>	Cd(II)	8.46	54
<i>Caulerpa lentillifera</i>	Cd(II)	4.69	55
<i>A. tumefaciens</i> 12b3	Cd(II)	56.17	This strain

increasing value of contact time till 30 min beyond which no further adsorption take place and state of equilibrium is established. Adsorption increases with increase in concentration of metal, maximum adsorption occurring at 150 mg L^{-1} . Langmuir isotherm and Pseudo-second-order model

proved to be the best to describe the kinetics of adsorption whereas intra-particle diffusion was also involved in the adsorption of Cd(II) onto *A. tumefaciens* without limiting its rate. Over all, the novel bacterium *A. tumefaciens* has the capacity to remove cadmium as high as 56.17 mg g^{-1} in the solution. This study concludes that endophytic *A. tumefaciens* possesses a good potential for heavy metal biosorption from wastewater and can be used for large scale applications.

References

- [1] S. Kim, Y. Cheong, D. Seo, J. Hur, J. Heo, J. Cho, Characterisation of heavy metal tolerance and biosorption capacity of bacterium strain CPB4 (*Bacillus* spp.), *Water Sci. Technol.*, 55 (2007) 105–111.
- [2] T. Anirudhan, S. Sreekumari, Adsorptive removal of heavy metal ions from industrial effluents using activated carbon derived from waste coconut buttons, *J. Environ. Sci.*, 23 (2011) 1989–1998.
- [3] A. Zouboulis, M. Loukidou, K. Matis, Biosorption of toxic metals from aqueous solutions by bacteria strains isolated from metal-polluted soils, *Proc. Biochem.*, 39 (2004) 909–916.
- [4] A.J.N. Kermani, M.F. Ghasemi, A. Khosravan, A. Farahmand, M. Shakibaie, Cadmium bioremediation by metal-resistant mutated bacteria isolated from active sludge of industrial effluent, *Iran, J. Envir. Health. Sci. Eng.*, 7 (2010) 279–286.
- [5] P. Banjerdki, P. Vattanaviboon, S. Mongkolsuk, Exposure to cadmium elevates expression of genes in the OxyR and OhrR regulons and induces cross-resistance to peroxide killing treatment in *Xanthomonas campestris*, *Appl. Environ. Microbiol.*, 71 (2005) 1843–1849.
- [6] D. Ghosh, R. Saha, A. Ghosh, R. Nandi, B. Saha, A review on toxic cadmium biosorption from contaminated wastewater, *Desal. Water Treat.*, 53 (2015) 413–420.
- [7] M. Lasfer, N. Vadrot, L. Aoudjehane, F. Conti, A. Bringuier, G. Feldmann, F. Reyl-Desmars, Cadmium induces mitochondria-dependent apoptosis of normal human hepatocytes, *Cell Biol. Toxicol.*, 24 (2008) 55–62.
- [8] G. Bertin, D. Averbek, Cadmium: cellular effects, modifications of biomolecules, modulation of DNA repair and genotoxic consequences (a review), *Biochimie.*, 88 (2006) 1549–1559.
- [9] X. Xiao, S. Luo, G. Zeng, W. Wei, Y. Wan, L. Chen, H. Guo, Z. Cao, L. Yang, J. Chen, Biosorption of cadmium by endophytic fungus (EF) *Microsphaeropsis* sp. LSE10 isolated from cadmium hyperaccumulator *Solanum nigrum* L, *Bioresour. Technol.*, 101 (2010) 1668–1674.
- [10] G. Chen, G. Zeng, L. Tang, C. Du, X. Jiang, G. Huang, H. Liu, G. Shen, Cadmium removal from simulated wastewater to biomass byproduct of *Lentinus edodes*, *Bioresour. Technol.*, 99 (2008) 7034–7040.
- [11] S.S. Ahluwalia, D. Goyal, Microbial and plant derived biomass for removal of heavy metals from wastewater, *Bioresour. Technol.*, 98 (2007) 2243–2257.
- [12] C. Mack, B. Wilhelm, J. Duncan, J. Burgess, Biosorption of precious metals, *Biotechnol. Adv.*, 25 (2007) 264–271.
- [13] F. Pagnanelli, S. Mainelli, L. Borneroni, D. Dionisi, L. Toro, Mechanisms of heavy-metal removal by activated sludge, *Chemosphere*, 75 (2009) 1028–1034.
- [14] A.M. Farhan, N.M. Salem, L.A. Ahmad, A.M. Awwad, Kinetic, equilibrium and thermodynamic studies of the biosorption of heavy metals by *Ceratonia siliquabark*, *Am. J. Chem.*, 2 (2012) 335–342.
- [15] A. Witek-Krowak, R.G. Szafran, S. Modelski, Biosorption of heavy metals from aqueous solutions onto peanut shell as a low-cost biosorbent, *Desalination*, 265 (2011) 126–134.
- [16] H.J. Chaudhary, G. Peng, M. Hu, Y. He, L. Yang, Y. Luo, Z. Tan, Genetic diversity of endophytic diazotrophs of the wild rice, *Oryza alta* and identification of the new diazotroph, *Acinetobacter oryzae* sp. nov, *Microb. Ecol.*, 63 (2012) 813–821.

- [17] R.A. Gillani, N. Shenaz, S. Matloob, F. Haq, W.S.W. Ngah, W. Nasim, M.F.H. Munis, A. Rehman, H.J. Chaudhary, Biosorption of Cr(III) and Pb(II) by endophytic *Agrobacterium tumefaciens* 12b3: equilibrium and kinetic studies, *Desal. Water Treat.*, 67 (2017) 206–214.
- [18] S.T. Akar, S. Arslan, T. Alp, D. Arslan, T. Akar, Biosorption potential of the waste biomaterial obtained from *Cucumis melo* for the removal of Pb²⁺ ions from aqueous media: equilibrium, kinetic, thermodynamic and mechanism analysis, *Chem. Eng. J.*, 185 (2012) 82–90.
- [19] F. Ghorbani, H. Younesi, S.M. Ghasempouri, A.A. Zinatizadeh, M. Amini, A. Daneshi, Application of response surface methodology for optimization of cadmium biosorption in an aqueous solution by *Saccharomyces cerevisiae*, *Chem. Eng. J.*, 145 (2008) 267–275.
- [20] R. Chakravarty, P.C. Banerjee, Mechanism of cadmium binding on the cell wall of an acidophilic bacterium, *Bioresour. Technol.*, 108 (2012) 176–183.
- [21] R. Say, A. Denizli, M.Y. Arica, Biosorption of cadmium (II), lead (II) and copper (II) with the filamentous fungus *Phanerochaete chrysosporium*, *Bioresour. Technol.*, 76 (2001) 67–70.
- [22] Y. Liu, Q. Cao, F. Luo, J. Chen, Biosorption of Cd²⁺, Cu²⁺, Ni²⁺ and Zn²⁺ ions from aqueous solutions by pretreated biomass of brown algae, *J. Hazard. Mater.*, 163 (2009) 931–938.
- [23] N. Dursun, M.M. Özcan, G. Kaşık, C. Öztürk, Mineral contents of 34 species of edible mushrooms growing wild in Turkey, *J. Sci. Food Agric.*, 86 (2006) 1087–1094.
- [24] N. Abdel-Ghani, M. Hefny, G.A. El-Chaghaby, Removal of lead from aqueous solution using low cost abundantly available adsorbents, *Int. J. Environ. Sci. Technol.*, 4 (2007) 67–73.
- [25] A. Zouboulis, M. Loukidou, K. Matis, Biosorption of toxic metals from aqueous solutions by bacteria strains isolated from metal-polluted soils, *Process Biochem.*, 39 (2004) 909–916.
- [26] R. Gabr, S. Hassan, A. Shoreit, Biosorption of lead and nickel by living and non-living cells of *Pseudomonas aeruginosa* ASU 6a, *Int. Biodeterior. Biodegrad.*, 62 (2008) 195–203.
- [27] V. Dang, H. Doan, T. Dang-Vu, A. Lohi, Equilibrium and kinetics of biosorption of cadmium (II) and copper (II) ions by wheat straw, *Bioresour. Technol.*, 100 (2009) 211–219.
- [28] T. Akar, Z. Kaynak, S. Ulusoy, D. Yuvaci, G. Ozsari, S.T. Akar, Enhanced biosorption of nickel (II) ions by silica-gel-immobilized waste biomass: biosorption characteristics in batch and dynamic flow mode, *J. Hazard. Mater.*, 163 (2009) 1134–1141.
- [29] V.K. Gupta, A. Rastogi, A. Nayak, Biosorption of nickel onto treated alga (*Oedogonium hatei*): application of isotherm and kinetic models, *J. Colloid Interface Sci.*, 342 (2010) 533–539.
- [30] H. Freundlich, Over the adsorption in solution, *J. Phys. Chem.*, 57 (1906) 385–470.
- [31] S.S. Gupta, K.G. Bhattacharyya, Kinetics of adsorption of metal ions on inorganic materials: a review, *Adv. Coll. Int. Sci.*, 162 (2011) 39–58.
- [32] M.A. Hubbe, K.R. Beck, W.G. O'Neal, Y.C. Sharma, Cellulosic substrates for removal of pollutants from aqueous systems: A review. 2, *Dyes, Bio. Resour.*, 7 (2012) 2592–2687.
- [33] Y. Ho, Comment on “Cadmium removal from aqueous solutions by chitin: Kinetic and equilibrium studies”, *Water Res.*, 38 (2004) 2962–2964.
- [34] Z. Reddad, C. Gerente, Y. Andres, P. Le Cloirec, Adsorption of several metal ions onto a low-cost biosorbent: kinetic and equilibrium studies, *Environ. Sci. Technol.*, 36 (2002) 2067–2073.
- [35] Y.S. Ho, Review of second-order models for adsorption systems, *J. Hazard. Mater.*, 136 (2006) 681–689.
- [36] M. Alkan, Ö. Demirbaş, M. Doğan, Adsorption kinetics and thermodynamics of an anionic dye onto sepiolite, *Micropor. Mesopor. Mat.*, 101 (2007) 388–396.
- [37] W. Weber, J. Morris, Kinetics of adsorption on carbon from solution, *J. Sanit. Eng. Div. Am. Soc. Civ. Eng.*, 89 (1963) 31–60.
- [38] R. Davis, L. Mauer, Fourier transform infrared (FT-IR) spectroscopy: a rapid tool for detection and analysis of foodborne pathogenic bacteria, *Curr. Res., Technol. Edu. topics in Appl. Microbiol. Microbial Biotechnol.*, 2 (2010) 1582–1594.
- [39] F.A. Pavan, A.C. Mazzocato, R.A. Jacques, S.L. Dias, Ponkan peel: a potential biosorbent for removal of Pb (II) ions from aqueous solution, *Biochem. Eng. J.*, 40 (2008) 357–362.
- [40] M. Fereidouni, A. Daneshi, H. Younesi, Biosorption equilibria of binary Cd (II) and Ni (II) systems onto *Saccharomyces cerevisiae* and *Ralstonia eutropha* cells: Application of response surface methodology, *J. Hazard. Mater.*, 168 (2009) 1437–1448.
- [41] M. Safari, A. Sorooshzadeh, A. Asgharzadeh, S. Saadat, The application of adsorption modeling and Fourier transform infrared spectroscopy to the comparison of two species of plant growth-promoting rhizobacteria as biosorbents of cadmium in different pH solutions, *Biorem. J.*, 17 (2013) 201–211.
- [42] X. Zeng, X. Liu, P. Jiang, W. Li, J. Tang, Cadmium removal by *Pseudomonas aeruginosa* E1, in: *Energy and Environment Technology, ICEET'09. International Conference on, IEEE*, (2009) 468–471.
- [43] G. Akkaya, F. Güzel, Bioremoval and recovery of Cu (II) and Pb (II) from aqueous solution by a novel biosorbent watermelon (*Citrullus lanatus*) seed hulls: kinetic study, equilibrium isotherm, SEM and FTIR analysis, *Desal. Water Treat.*, 51 (2013) 7311–7322.
- [44] E. Rusu, S. Jurcoane, G. Rusu, Rapid evaluation by UV-Vis and FT-IR spectroscopy of DINOCAP residue in soil: Microbiological implications, *Rom Biotechnol. Lett.*, 15 (2010).
- [45] J. Pan, X. Ge, R. Liu, H. Tang, Characteristic features of *Bacillus cereus* cell surfaces with biosorption of Pb (II) ions by AFM and FT-IR, *Colloids and surfaces B: Biointerfaces*, 52 (2006) 89–95.
- [46] M. Safari, A. Sorooshzadeh, A. Asgharzadeh, S. Saadat, The application of adsorption modeling and Fourier transform infrared spectroscopy to the comparison of two species of plant growth-promoting rhizobacteria as biosorbents of cadmium in different pH solutions, *Biorem. J.*, 17 (2013) 201–211.
- [47] G. Naja, C. Mustin, B. Volesky, J. Berthelin, A high-resolution titrator: a new approach to studying binding sites of microbial biosorbents, *Water Res.*, 39 (2005) 579–588.
- [48] V. Rajesh, A.S.K. Kumar, N. Rajesh, Biosorption of cadmium using a novel bacterium isolated from an electronic industry effluent, *Chem. Eng. J.*, 235 (2014) 176–185.
- [49] P. Arivalagan, D. Singaraj, V. Haridass, T. Kaliannan, Removal of cadmium from aqueous solution by batch studies using *Bacillus cereus*, *Ecol. Eng.*, 71 (2014) 728–735.
- [50] F. Ghorbani, H. Younesi, S.M. Ghasempouri, A.A. Zinatizadeh, M. Amini, A. Daneshi, Application of response surface methodology for optimization of cadmium biosorption in an aqueous solution by *Saccharomyces cerevisiae*, *Chem. Eng. J.*, 145 (2008) 267–275.
- [51] S.Ö. Zdemir, E. Kılınc, A. Poli, B. Nicolaus, Biosorption of Heavy Metals (Cd²⁺, Cu²⁺, Co²⁺, and Mn²⁺) by thermophilic bacteria, *Geobacillus thermantarcticus* and *Anoxybacillus amylolyticus*: Equilibrium and Kinetic Studies, *Bioremediat. J.*, 17 (2013) 86–96.
- [52] J. Nirmal Kumar, C. Oommen, Removal of heavy metals by biosorption using freshwater alga *Spirogyra hyalina*, *J. Environ. Biol.*, 33 (2012) 27–31.
- [53] T.G.P. Vasquez, A.E.C. Botero, L.M.S. de Mesquita, M.L. Torem, Biosorptive removal of Cd and Zn from liquid streams with a *Rhodococcus opacus* strain, *Miner. Eng.*, 20 (2007) 939–944.
- [54] G. Yan, T. Viraraghavan, Heavy-metal removal from aqueous solution by fungus *Mucor rouxii*, *Water Res.*, 37 (2003) 4486–4496.
- [55] P. Pavasant, R. Apiratikul, V. Sungkhum, P. Suthiparinyanont, S. Wattanachira, T.F. Marhaba, Biosorption of Cu²⁺, Cd²⁺, Pb²⁺, and Zn²⁺ using dried marine green macroalga *Caulerpa lentillifera*, *Bioresour. Technol.*, 97 (2006) 2321–2329.